Manufacturing highly potent CD20/CD19-targeted iCasp9 regulatable CAR-T cells using the *Quantum pBac-based CAR-T (qCART)* system for clinical application

Yi-Chun Chen[1,*], Peter S. Chang[1,*], Wei-Kai Hua[1], Jeff C. Hsu[1], Jui-Cheng Tsai[1], Yi-Wun Huang[1], Yi-Hsin Kao[1], Pei-Hua Wu[1], Yi-Fang Chang[2,3,4], Ming Chih Chang[2], Yu Cheng Chang[2,3], Kuo-Lan Karen Wen[1,†], Sareina Chiung-Yuan Wu[1,†]

[1]GenomeFrontier Therapeutics, Inc. Taipei City, Taiwan (R.O.C.)

[2]Division of Hematology and Oncology, Department of Internal Medicine, Mackay Memorial Hospital, Taipei, Taiwan (R.O.C.)

[3]Department of Medical Research, Laboratory of Good Clinical Research Center, Mackay Memorial Hospital, Tamsui District, New Taipei City, Taiwan (R.O.C.)

[4]Department of Medicine, Mackay Medical College, New Taipei City, Taiwan (R.O.C.)

[*]These authors contributed equally

[†]To whom correspondence may be addressed. Sareina Chiung-Yuan Wu, Kuo-Lan Karen Wen; 18F-1, No. 3, Park St., Nangang Dist., Taipei City 11503, Taiwan (R.O.C.); +886-2-26558766;

Email: sareina@genomefrontier.com, klwen@genomefrontier.com

Abstract

CD19-targeted chimeric antigen receptor therapies (CAR19) have driven a paradigm shift in the treatment of relapsed/refractory B-cell malignancies. However, >50% of CAR19-treated patients experienced progressive disease mainly due to antigen escape and low persistence. Clinical prognosis is heavily influenced by CAR-T cell function and systemic cytokine toxicities. Furthermore, it remains a challenge to efficiently, cost-effectively, and consistently manufacture clinically relevant number of virally engineered CAR-T cells. Using a highly efficient *piggyBac* transposon-based vector, *Quantum pBac*, we developed a virus-free cell engineering system, *Quantum CAR-T (qCART^{TM})*, for development and production of multiplex CAR-T therapies. Here, we demonstrated *in vitro and in vivo* that consistent, robust, and functional CD20/CD19 dual-targeted CAR-T stem cell memory (T_{SCM}) cells can be efficiently manufactured using the *qCART^{TM}* system for clinical application. *qCART^{TM}*-manufactured CAR-T cells from cancer patients expanded efficiently, rapidly eradicated tumors, and can be safely controlled via an iCasp9 suicide gene-inducing drug.

Introduction

T cells can be genetically engineered to express a chimeric antigen receptor (CAR) that targets cancer. Over the last decade, CAR-T therapy has become one of the most promising cancer treatment.[1] While successful clinical trials have sprung several biotech companies recently, the heavy reliance on lentiviral and retroviral vectors for the generation of clinically relevant number of CAR-T cells makes the therapy expensive and inaccessible to the masses. Safety concerns have been raised regarding the frequent cytokine release syndrome (CRS) and immune effector cell-associated neurotoxicity syndrome (ICANS) associated with clinical patients treated with conventional CAR-T therapies.[2] Furthermore, virus-based gene therapies have limited gene payload capacity, making them less suitable for engineering multiplex armored CAR-T cells to express multiple T cell-enhancing factors.[3,4]

To date, B-cell malignancies remain the most actively studied cancers for CAR-T therapy development. Since *Brentjens et al. (2003)* first demonstrated the eradication of B-cell tumors by CD19-targeted second generation CAR-T cells, several commercial CAR-T products (tisagenlecleucel T, axicabtagene ciloleucel, brexucabtagene autoleucel) have been approved by the FDA.[5,6] However, treatment with CD19-targeted CAR-T therapy resulted in only 30-40% long-term progression-free survival (PFS) in aggressive Non-Hodgkin lymphoma (NHL) patients, and the median 1-year event-free survival (EFS) of adult B-cell ALL patients was only 6.1 months with a median overall survival (OS) of 12.9 months.[7,8] Evidence suggest that downregulation of CD19 may in part be responsible for patient relapse.[9,10] As demonstrated by recent clinical studies, bispecific CD19 and CD20 dual-targeting CAR-T therapy significantly improved the survival of B-cell cancer patients compared to CD19 single-targeting CAR-T therapy.[11,12]

Transposon system is a virus-free alternative method for generating therapeutic CAR-T cells.[3,13] *Sleeping Beauty* and *piggyBac* are two transposon vector systems actively being tested in CAR-T clinical trials, but they suffer from low gene transfer efficiency and limited expansion of engineered cells.[14] We recently developed the most advanced version of *piggyBac* known as *Quantum pBac^{TM} (qPB)* that is 15 times more active and potentially safer than *hyperactive piggyBac* in human T cells[44,45]. In our previous studies, we successfully developed a novel genetic engineering system known as *Quantum CAR-T (qCART^{TM})* that combines efficient transgene design, evaluation, and identification of lead construct (*GTailor^{TM}*); virus-free vector (*Quantum pBac^{TM}*); effective gene delivery (*Quantum Nufect^{TM}*); and optimized cell

expansion (*iCellar*^{TM})[44,45]. We reported that *qCART*^{TM} could be generically used to engineer highly potent CAR-T stem cell memory (T_{SCM}), a T cell population associated with enhanced anti-tumor efficacy in cancer patients.[15] Here, we further validate that *qCART*^{TM} system can be used to manufacture highly potent bicistronic CD20/CD19-targeted iCasp9 regulatable CAR-T cells (GF-CART01) for treating B-cell malignancies. GF-CART01 cells can be rapidly expanded to clinically relevant number within 10 days post-nucleofection. We demonstrate enhanced anti-tumor efficacy of GF-CART01 cells both *in vitro* and in a xenotransplant immunodeficient mouse model. Finally, we establish the functionality of GF-CART01 cells in cancer patients. Together, these results support the therapeutic use of GF-CART01 therapy for clinical application. The robustness and consistency of the *qCART*^{TM} system make it possible for patient CAR-T cells to be manufactured efficiently and economically.

Results

Comparison of fed-batch (G-Rex) and perfusion (conventional)-cultured CAR-T cells

To assess the potential to develop CAR-T cell therapies using the *qPB* transposon system, we constructed a second-generation bicistronic CAR (GF-CART01) containing binding domains that recognize CD20 and CD19, human 4-1BB and CD3ζ signaling domains, and iCasp9 suicide gene driven by an EF1α promoter **(Figure 1A)**. Following nucleofection of GF-CART01 DNA, we expanded CAR-T cells in G-Rex (fed-batch) and conventional (perfusion) plates. The phenotype and effector functions of fed-batch- and perfusion-cultured CAR-T cells were compared. No significant difference was observed in the percentage of CAR^+ T cells in the fed-batch-cultured (46%) and perfusion-cultured (51%) CAR-T cells **(Figure 1B)**. After continuous culturing for 10 days, we observed significantly higher expansion of perfusion-cultured CAR-T cells (836 fold) compared to fed-batch-cultured CAR-T cells (189 fold). Notably, both the perfusion- and fed-batch-cultured CAR-T cells had a high percentage of $CD45RA^+CD62L^+CD95^+$ T memory stem cells (T_{SCM}) in both the CAR^+ CD4 and CD8 populations. Despite noticeable lower proliferation of fed-batch compared to perfusion-cultured CAR-T cells, we observed significantly enhanced anti-tumor cytotoxicity in fed-batch-cultured CAR-T cells 48 and 72 hours after co-culturing with Raji-GFP/Luc tumor **(Figure 1C)**. As G-Rex will be adopted for good manufacturing practice (GMP) CAR-T manufacturing, all subsequent experiments were conducted using fed-batch-cultured CAR-T cells.

Safety assessment of GF-CART01 cells

To better manage CAR-T cell therapy associated adversities, we included an iCasp9 suicide gene in the GF-CART01 construct, which resulted in the death of CAR-T cells upon AP1903 treatment **(Supplementary Figure 1A)**. We demonstrated that AP1903 had no significant effect on the survival of CAR-T cells that lacked the iCasp9 gene in the CAR construct. On the other hand, AP1903 treatment resulted in significant reduction in GF-CART01 cell survival.

To comply with GMP safety standards for CAR-T cell production, we need to ensure that GF-CART01 cells have low CAR copy number per cell (<5). We therefore modified CAR-T cells using different amounts of GF-CART01 DNA to determine the optimal amount to be used for CAR-T cell production. We have previously demonstrated that increasing the concentration of DNA for electroporation increased CAR^+ T cells in a dose-dependent manner (data not shown). Here we determined that, the CAR copy number remained low (<5) when 15 µg of total DNA was used for nucleofection **(Supplementary Figure 1B)**. All subsequent experiments were conducted using 15 µg of DNA per $5x10^6$ cells to maximize generation of CAR^+ T cells while maintaining safety levels of CAR DNA copy numbers.

GF-CART01 cells are dominated by T_{SCM} cells with high proliferative capacity and low expression of exhaustion and senescence markers

To examine the proliferative capacity of GF-CART01 cells, we used the *qCART*^{TM} system to generate CAR-T cells from 9 independent healthy donors and monitored CAR expression on days 1, 8, and 10 following nucleofection. We observed a mean basal level of around 21.49% CAR$^+$ T cell population on day 1, which subsequently increased and stabilized around 55.7% and 56.75% on days 8 and 10, respectively **(Figure 2A)**. As the presence of transposase (Quantum pBase) in modified T cells may lead to genotoxicity long-term, we also monitored the Quantum pBase levels following nucleofection. While the Quantum pBase levels were high on day 1 (47.31%), only a minimal (<0.2%) fraction of Quantum pBase$^+$ cells was observed on days 8 and 10, suggesting that concerns regarding Quantum pBase-induced integrant remobilization should be minimal **(Figure 2B).** Quantifying the total expansion of GF-CART01 cells, we saw an average of about 178.86-fold CAR-T cell expansion **(Figure 2C)**.

Among the 9 donors, we also consistently observed a higher CD8 (73.58%) population in the GF-CART01 cells compared to the CD4 (21.98%) population **(Figure 2D)**. To better understand the composition of GF-CART01 cells, we assessed the expression of CD45RA, CD62L, and CD95 in the CD4 and CD8 CAR$^+$ populations to determine the percentage of CD45RA$^+$CD62L$^+$CD95$^-$ naïve T cell (T_N), CD45RA$^+$CD62L$^+$CD95$^+$ stem cell memory T cell (T_{SCM}), CD45RA$^-$CD62L$^+$CD95$^+$ central memory T cell (T_{CM}), CD45RA$^-$CD62L$^-$CD95$^+$ effector memory T cell (T_{EM}), and CD45RA$^-$CD62L$^-$CD95$^-$ effector T cell (T_{EFF}) subsets. We observed high percentage of T_{SCM} CAR-T cells in both the CD4 (68.94%) and CD8 (79.84%) populations compared to the other T cell subsets **(Figure 2E)**. Furthermore, these CAR-T cells display low exhaustion (PD-1, TIM-3, and LAG-3) marker and the senescence marker CD57 expression **(Figure 2F and G)**. Interestingly, a small but significant population (~9.92%) expressed the senescence marker KLRG-1.

GF-CART01 cells display robust cytotoxic function and secrete pro-inflammatory cytokines

We next tested the anti-tumor function of GF-CART01 cells in two independent donors, PBMC-41 and PBMC-40. Raji-GFP/Luc tumor cells were co-cultured with GF-CART01 cells at effector to target (E:T) ratios of 5:1, 1:1, and 1:5, and cytotoxicity was assessed at 24, 48, 72, and 96 hours after co-culture **(Figure 3A and B)**. At early time points (24 to 48 h), we observed that GF-CART01 cells lysed Raji tumors in a dose-dependent manner. On the other hand, complete tumor lysis was seen in all E:T ratios at 96 hours. Furthermore, we assessed the secretion of pro-inflammatory cytokines IFN-γ, TNF-α, and IL-2 in the co-culture supernatants. In both donors, GF-CART01 cells secreted significant levels of IFN-γ, TNF-α, and IL-2 compared to pan-T cells **(Figure 3C-E)**. Collectively, these data suggest that functional GF-CART01 CAR-T cells can be generated using the *qCART*^{TM} system.

GF-CART01 cells display enhanced and persistent anti-tumor function *in vivo*

We next evaluated the anti-tumor efficacy of GF-CART01 cells in an *in vivo* xenotransplant immunodeficient mouse model using donor PBMC-41. We injected $1.5x10^5$ Raji GFP/Luc tumor cells intravenously (i.v.) followed by $5.5x10^5$ (low), $3.0x10^6$ (medium), or $1x10^7$ (high) GF-CART01 cells (i.v.) 7 days later as depicted in **Figure 4A**. As a control, we included four additional mice that were infused with Raji-GFP/Luc tumor cells and lacked GF-CART01 cell treatment (vehicle). Tumor burden was assessed weekly via bioluminescence **(Figure 4B-C)**. All mice in the vehicle treatment group succumbed to tumor by day 21. On the other hand, all Raji tumors were completely eradicated by day 13 in all three treatment groups and remained tumor-free as late as day 34 **(Figure 4B)**. Eye bleeding was performed on days 2, 5, 8, and 14 to assess cytokine production, and day 26 to assess persistence of CAR-T cells and Raji tumors. No significant levels of cytokine production were detected in all three treatment groups on days 2, 8, and 14 **(Figure 4E)**. On day 26, no detectable levels of Raji-GFP/Luc tumors were observed in all three GF-CART01 treatment groups as assessed by the lack of luciferase gene detected in the blood

(Figure 4F). Moreover, residual CAR gene was observed in the blood of the medium and high treatment groups, suggesting that many GF-CART01 cells persisted to form memory T cells **(Figure 4G)**.

While GF-CART01 cells persisted as late as day 26 post-treatment, it remained unclear whether these residual cells were memory T cells and retained their anti-tumor function. To address this issue, we rechallenged half of the mice in each treatment group with $1.5x10^5$ Raji GFP/Luc tumor cells on day 35. Due to the lack of CAR-T cell persistence, most of the rechallenged mice in the low treatment group eventually succumbed to tumor **(Figure 4B-C)**. In contrast, the rechallenged mice in the medium and high treatment groups remained tumor-free throughout the *in vivo* experiment. Some mice in the medium and high treatment groups did not survive, but this was likely due to graft-versus-host disease (GVHD) as severe ruffling were observed in these mice. More importantly, GF-CART01 cell treatment significantly improved the overall survival of tumor-bearing mice compared to the vehicle control group **(Figure 4D)**.

Functional GF-CART01 T_{SCM} cells can be generated in sufficient number from cancer patients

We have thus far demonstrated the enhanced anti-tumor efficacy of GF-CART01 cell therapy both *in vitro* and *in vivo*. However, it is important to assess whether sufficient high quality GF-CART01 cells can be generated for clinical applications. In our previous experiments thus far, we expanded all GF-CART01 cells with CD19-expressing artificial antigen presenting cells (aAPC). To streamline the manufacturing process, we tested whether we can still generate highly potent patient-derived GF-CART01 T_{SCM} cells in the absence of aAPC selective expansion. We isolated PBMCs from 6 healthy donors, 3 diffuse large B-cell lymphoma (DLBCL) patients, 3 chronic lymphocytic leukemia (CLL) patients, one Hodgkin lymphoma (HL) patient, and one multiple myeloma patient to generate GF-CART01 cells. **Figure 5** and **Table 1** summarize the characteristics of the CAR-T cells generated from the healthy donors and patients. Over the course of 10 days, we expanded the CAR-T cells to $4.58x10^6$–$2.754x10^7$ cells in a 24-well G-Rex culture, which would be equivalent to clinically relevant number of $2.29x10^8$–$1.38x10^9$ cells in a 1L G-Rex culture vessel. The CAR expression (19.9–53.22%) and the fold expansion (58.0–198.96 folds) of the patient cells were comparable to those from healthy donors (32.5–49.6% and 43.54–157.55 folds) **(Table 1)**. The purity of the engineered CAR-T cells was confirmed by the low percentage of $CD19^+$ B cells and $CD3^-CD56^+$ NK cells in both the healthy donors (0.01-0.36% B; 0.04-0.27% NK) and patient cells (0-1.18% B; 0.02-2.69% NK) **(Table 1)**. The proportion of CD8 and CD4 were relatively even among both the healthy donors (CD8/CD4=0.85) and the patients (1.17) prior to nucleofection **(Figure 5A)**. After nucleofection, the GF-CART01 CAR^+ cells from healthy donors had higher CD8/CD4 ratio (5.64). However, the increase in the proportion of CAR^+ CD8 T cells was only observed in some patients **(Figure 5A)**. Notably, compared to pre-nucleofection levels, the percentages of T_{SCM} subset at 10 days post-nucleofection demonstrated a substantial increase in all patients among the CD4 (from 13.75% to 76.25%) and CD8 (from 7.17% to 81.90%) populations, confirming the unique quality of *qCART™* system in supporting T_{SCM} differentiation **(Figure 5B)**. Consistent with our previous experiments, the GF-CART01 cells were characterized by low expression of exhaustion markers PD-1 and TIM-3, and senescence marker CD57 **(Table 1)**. The expression of the exhaustion marker LAG-3 was low in CLL, HL, and MM patients (2.4-4%) with slightly elevated expression among the DLBCL patients (9.9-22.8%). While KLRG-1 expression (~7.25%) was detectable in GF-CART01 patient cells, it was significantly lower than KLRG-1 expression prior to CAR nucleofection (~21.27%; p=0.0087) **(Supplementary Figure 2A)**. The decrease in KLRG-1 expression after nucleofection was especially prominent in the CD8 population (52.50% vs. 14.59%; p=0.0004) **(Supplementary Figure 2B)**. A 48-hour cytotoxicity assay further confirmed the functionality of the GF-CART01 cells **(Table 1)**. Together, our data suggest that the *qCART™* system is a promising technology for generating functional multiplex armored CAR-T_{SCM} cells for cancer

immunotherapy application. We demonstrated that GF-CART01 therapy is a safe, potent, and cost-effective treatment for B-cell malignancies.

Discussion

Quantum pBac^{TM} is currently the most efficient transposon for gene integration, and GF-CART01 cell therapy was our first CAR-T therapy using the novel *qPB*-based *qCART*^{TM} system[44,45]. The *qCART*^{TM} system can easily produce CAR-T cells with transgene size >7.6 kb[45], which is not achievable by conventional lentiviral/retroviral CAR-T engineering. This limited cargo capacity may account for the lack of current CAR-T clinical trials targeting B-cell malignancies with both dual-targeting and iCasp9 safety switch gene (5.2 Kb transgene size) in the CAR design. In this report, we presented strong evidence on the feasibility of manufacturing highly potent iCasp9-regulatable CD20/CD19-targeted CAR-T_{SCM} cells using the virus-free *qCART*^{TM} system for clinical application. We demonstrated the superior safety, purity, potency, and consistency profiles of CAR-T cells manufactured using the *qCART*^{TM} system.

Maintaining sterility and controlling mycoplasma and endotoxin contamination in the CAR-T product are of utmost importance for safe manufacturing. G-Rex is a GMP-compliant medical device used for T cell expansion.[16,17] The minimal manual operation of this device reduces contamination risks compared to perfusion-cultured flask. Importantly, we demonstrated that manufacturing GF-CART01 cells with G-Rex can be achieved without compromising CAR-T efficacy **(Figure 1)**. Genotoxicity is also a predominant safety issue associated with gene therapy products. Consistent with our previous study, we observed low risk of genotoxicity in *qCART*^{TM}-manufactured CAR-T cells, given the low integrant copy number, safe integration profile, low enhancer activity, and low residual Quantum pBase, suggesting minimal integrant remobilization risks[45]**(Supplementary Figure 1B; Figure 2B**). Furthermore, acute toxicities in patients in response to CAR-T therapies, such as CRS and ICANS, have been major concerns in CAR-T development.[18–20] Furthermore, CAR-T cells have the potential to transform into cancer cells; a rare case of CAR^+ CD4 T cell lymphoma has been reported recently in patients treated with CD19 CAR-T cells.[21,22] To safely manage toxicities, CAR-T cells can be eradicated by targeting CAR-T cells (e.g. anti-EGFRt antibody) via antibody-dependent cellular cytotoxicity (ADCC) mechanism or using a small molecule that activates a suicide gene introduced in the CAR design (e.g. iCasp9).[18] The ADCC approach has slower onset of killing compared to the latter. Recently, Foster et al (2021) has demonstrated that acute ICANS can be effectively controlled by treating CAR-T therapy patients with the iCasp9-activating agent, rimiducidn.[23] We included an iCasp9 safety switch in our GF-CART01 design to mitigate the tumorigenicity risk associated with genetic manipulation, and we confirmed that CAR-T cells can be eliminated upon AP1903 drug treatment.

Manufacturing clinically relevant number of a pure high-quality CAR-T product is the first critical step towards successful CAR-T therapy. One approach to expanding the population of CAR^+ T cells is by culturing in aAPC, but this often leads to a more differentiated and short-lived T_{EFF} or exhaustive CAR-T phenotypes.[24] Another approach is to include markers within the construct to enrich the CAR^+ T cell population either via drug selection or antibody-mediated cell isolation during or after CAR-T *ex vivo* expansion, respectively. However, such approaches increase the payload size and introduce therapeutically irrelevant genes into the genome.[4,19,20] While we also used aAPC in our initial experiments, we could generate sufficient quantity of patient-derived *qCART*^{TM}-modified CAR-T cells without aAPC-induced enrichment. Our recent study further confirmed that *qCART*^{TM}-manufactured CAR-T cells may be more effective in tumor control without aAPC enrichment[45]. Here, we demonstrated that $2.29x10^8$–$1.38x10^9$ T cells could be generated in a 1 L-G-Rex within a short time-frame of 12 days using T cells from patients with B-cell malignancies. We validated the purity of the CAR-T cell population by showing minimal B and NK cell contamination **(Table 1)**. Even at a low transfection efficiency of 20%, we could still produce sufficient number of CAR-T cells ($4.58x10^7$–$2.76x10^8$) for treatment, and we can easily achieve higher percentages of CAR^+ T cells by using aAPC should the need arise.

Regarding the potency of manufactured cells, we demonstrated *in vitro* and *in vivo* that GF-CART01 therapy is highly effective in eradicating B-cell malignancies **(Figure 3-4)**. The high potency of GF-CART01 cells can be attributed to the balance of CD8/CD4 CAR-T ratio and the high enrichment of T_{SCM} in the engineered cells. It has been reported that a balanced CD8/CD4 CAR-T ratio resulted in high remission rates.[25,26] To achieve this, others have engineered CD4 and CD8 CAR-T cells separately before adoptive transfer.[25] While *qCART™* cells derived from healthy donors generally favored CD8 enrichment, *qCART™* cells derived from cancer patients have a balanced CD8/CD4 CAR-T ratio (**Figure 5)**. Thus, the *qCART™* system naturally achieves the desired CD8/CD4 balance without the need to engineer CD4 and CD8 CAR-T cells separately as seen in SB100X-modified CAR-T clinical trials.[27]

T_{SCM} are a class of immunological memory that have been identified as a T cell subset critical for successful adoptive T cell therapies.[15,28–31] *qCART™* system differentiates from other gene modification systems in its ability to enrich T_{SCM} population without compromising the cell quality, expansion, and production time of the CAR-T cell product[45]. One approach to harness the potency of less-differentiated T cells such as T_{SCM} is to shorten the *ex vivo* expansion time of CAR-T product. *Ghassemi et al.* (2022) demonstrated that shortening the lentiviral CAR-T manufacturing process to 24-hours resulted in higher percentage of CAR-T cells with a memory phenotype.[32] Though these CAR-T cells displayed stronger *in vivo* anti-tumor activity than their conventional counterpart, it remains to be seen whether such a rapid manufacturing process can be successfully translated into a clinical setting. Another approach is to culture CAR-T cells in the presence of specific cytokines or chemical reagents.[30,31,33–35] Additionally, CAR-T cell production from defined T cell subsets has recently been shown to be very beneficial in enriching the T_{SCM} population.[36] However, none of these approaches enrich T_{SCM} population to a high level seen in our *qCART™*-modified T cells. While T_{SCM} cells make up a small percentage of T cells derived from cancer patients, genetically modifying these cells using the *qCART™* system resulted in enrichment of T_{SCM} to as high as >80% in both the CD4 and CD8 T cell populations **(Figure 5B)**.

In conjunction with the ability of T_{SCM} to self-renew and persist long-term, we also observed low expression of exhaustion (PD-1, TIM-3, and LAG-3) and senescence (CD57) biomarkers in our GF-CART01 cells **(Figure 2F-G; Table 1)**. KLRG1 is a marker associated with senescence. While we observed a small but significant population of KLRG-1^+ cells in GF-CART01 CAR-T cells, we also observed a significantly lower percentage of KLRG-1^+ cells after CAR-T production compared to freshly isolated PBMCs **(Supplementary Figure 2)**. Herndler-Brandstetter *et al.* (2018) recently described a class of memory T cell population developed from KLRG1^+ effector CD8 T cells that have lost KLRG1 expression.[37] These so-called "exKLRG1 memory cells" have been demonstrated to inhibit tumor growth more efficiently compared to KLRG1^+ cells in an OT-I melanoma mouse model. T_{SCM} cells generally lack KLRG1 expression, and KLRG1^+ T_{SCM} cells have been associated with cancer patients undergoing relapse.[38,39] Given the significant decrease in KLRG1 expression in GF-CART01 cells, it is possible that a significant proportion of CAR-T_{SCM} cells in our model were actually exKLRG1 memory cells. Thus, one possible mechanism that made it possible for *qCART™* system to generate highly potent CAR-T_{SCM} cells may be through the conversion of KLRG1^+ effector CD8 T cells to exKLRG1 memory cells.

One of the major challenges of CAR-T cell manufacturing is the variation and inconsistency of CAR-T cell products.[40] In one study of ten CLL and ALL patients, CAR-T cells expanded anywhere between 23.6 and 385-folds with retroviral CAR transduction of 4-70%.[41] Lentiviral transduction of 5.5-45.3% was reported by other studies of CLL and ALL patients.[42,43] In our GF-CART01 study, we observed tighter range of CAR$^+$ percentage (19.9-53.22%) and expansion (58.0-198.96 folds) among the eight cancer patients **(Table 1)**. Furthermore, these low levels of variation were comparable to the CAR$^+$ percentage (32.5-49.6%) and

expansion (43.54-157.55 folds) among the nine healthy donors in our study, respectively. More importantly, we demonstrated that GF-CART01 cells derived from both healthy donors and patients can effectively eradicate tumor cells **(Figure 3, Table 1)**.

The *qCART*^{TM} system is an elegant system for the manufacturing of CAR-T products. It has the unique ability to expand CAR-T_{SCM} to clinically relevant numbers in a timely and consistent fashion without compromising quality. Moreover, manufacturing using the *qCART*^{TM} system compared to lentiviral/retroviral vector systems reduces cost significantly.[40] In this study, we demonstrated that the qCART^{TM} system can be used to produce patient-derived GF-CART01 cells with all the desired CAR-T therapy attributes, including high CAR-$T_{SCM,}$ balanced CD8/CD4 ratio, low exhaustion and senescence marker expressions, high expansion capacity, and excellent anti-tumor efficacy. We believe that the simplicity of manufacturing multiplex CAR-T cells using the *qCART*^{TM} system will not only significantly enhance the accessibility of CAR-T therapy but also unlock the full potential of armored CAR-T therapy for the treatment of solid tumors in the future.

Materials and Methods

Generation and expansion of CAR-T cells

Fresh and frozen peripheral blood mononuclear cells (PBMCs) from adult healthy donors were obtained from Chang Gung Memorial Hospital (Linkou, Taiwan), the acquisition of samples was approved by the Institution Review Board (IRB No. 201900578A3) at Chang Gung Medical Foundation (For patient samples: IRB No. 20MMHIS330e, MacKay Memorial Hospital). Peripheral blood mononuclear cells (PBMCs) were extracted using Ficoll-Hypaque gradient separation (Cytiva). Primary human $CD3^+$ T cells were isolated from PBMCs by EasySep™ Human T Cell Isolation Kit (StemCell Technologies) or by Dynabeads™ Human T-Expander CD3/CD28 (Thermo Fisher Scientific). T cells were activated for two days using Dynabeads™ at a 3:1 bead to cell ratio. An iCasp9-CD20/CD19-CAR transposon minicircle and a Quantum pBase™ plasmid were delivered into activated T cells using 4D-Nucleofector device (Lonza) and Quantum Nufect Kit (GenomeFrontier Therapeutics) according to the manufacturer's instructions. Irradiated artificial antigen presenting cells (aAPC), CD19-expressing K562 cells, were added to electroporated T cells at 1:1 ratio on day 3. Cells were cultured in OpTmizer medium (Thermo Fisher) supplemented with Quantum Booster™ (GenomeFrontier Therapeutics) in G-Rex 24- or 6M-well plates (Wilson Wolf) or conventional plates for 10 days.

Flow cytometry

Surface expression of CAR on T cells was analyzed by co-incubating cells with a Biotin-SP (long spacer) AffiniPure Goat Anti-Mouse IgG, $F(ab')_2$ fragment specific antibody (Jackson ImmunoResearch) for 30 minutes at 4°C. Cells were then washed in FACS buffer followed by co-incubating cells with R-phycoerythrin (PE)-conjugated streptavidin (Jackson ImmunoResearch) for 30 minutes at 4°C. T cells were stained with fluorescent-labeled antibodies: CD4-Alexa Flour 532 (Thermo Fisher Scientific), CD3-Pacific Blue, CD4-Alexa Fluor 532, CD8-PE-Cy7, CD45RA-BV421, CD62L-PE-Cy5, CD95-BV711, CD279 (PD-1)-PE/Cy7, CD366 (Tim-3)-BV650, CD223 (LAG-3)-BV711, KLRG1-BV-421, CD57-PerCP-Cy5.5 (BioLegend). Flow cytometric analysis was performed on an SA3800 Spectral Analyzer (Sony). The graphs were generated using GraphPad Prism (GraphPad Software).

Enzyme-linked immunosorbent assay (ELISA)

For *in vitro* cytokine release assay, CAR-T cells were co-cultured with target tumor cells Raji GFP/Luc at E:T ratio of 1:1 for 24 hours before the culture supernatant was collected. For *in vivo* cytokine release assay, mouse sera samples were collected on day 2, 5, 8, and 14 after T cell injection. The presence of IFN-γ (Thermo Fisher), TNF-α (Thermo Fisher), IL-6 (Thermo Fisher), and IL-2 (BioLegend) was quantified by ELISA according to manufacturer's instructions.

Genomic DNA extraction and quantitative PCR (qPCR)

Genomic DNA from mouse blood was extracted using a DNeasy Blood & Tissue Kit (Qiagen) following the manufacturer's instructions. For qPCR analysis, the CAR and Luciferase genes represent CAR-T cells and Raji GFP/Luc cells, respectively. The following primer sequences were

used: CAR: Forward primer 5'-ACGTCGTACTCTTCCCGTCT-3'; Reverse primer: 5'-GATCACCCTGTACTGCAACCA-3'; Luciferase: Forward primer 5'-GGACTTGGACACCGGTAAGA-3'; Reverse primer: 5'-GGTCCACGATGAAGAAGTGC-3'. All qPCR assays were performed using a 7500 fast real-time PCR system (Applied Biosystems). Absolute levels of the transgenes were calculated using the standard curve method. Standard DNA fragments of CAR and Luciferase used its own plasmid DNA which was serially diluted for each standard curve, and the serially diluted solution was amplified with each gene-specific primer pair and mouse genomic DNA. The threshold cycle (CT) value of each target was converted to a concentration using the appropriate standard curve followed by calculating the % of cells in mouse blood based on the copy number of cells.

***In vitro* cytotoxicity assay**

Imaging of CAR-T cell cytotoxicity was performed using Celigo image cytometry (Nexcelom). The target cell line Raji-GFP/Luc was seeded in 96 well culture plates. T cells were then added at E:T ratios of 5:1, 1:1, and 1:5. At 0, 24, 48, 72, and 96 hours after co-culturing of Raji-GFP/Luc and CAR-T cells, the number of Raji-GFP/Luc cells remained were counted. Cell aggregates were separated by pipetting before imaging. The percent of specific lysis was calculated from each sample using the formula [1-(live fluorescent cell count in target cells with effector cell co-culturing/ live fluorescent cell count in target cells without effector cell co-culturing)] x 100.

Anti-tumor efficacy in mouse tumor models

In vivo studies using mouse xenograft model were conducted at the Development Center for Biotechnology, Taiwan, using animal protocols approved by the Taiwan Mouse Clinic IACUC (2020-R501-035). Eight-week-old male immunodeficient (NOD.Cg-Prkdc^{scid}Il2rg^{tm1Wjl}/YckNarl) mice (National Laboratory Animal Center, Taiwan) were engrafted with 1.5 x 10^5 Raji-Luc/GFP tumor cells intravenously (i.v.). One week after infusion, mice were infused with 7.5 x 10^5 (low), 3 x 10^6 (medium) or 1 x 10^7 (high) CAR-T cells from donor PBMC-41. After 35 days, 1.5 x 10^5 Raji-Luc/GFP tumor cells were injected (i.v.) to half of the mice that had been injected with CAR-T cells. Signals from infused Raji-Luc/GFP tumor cells were quantified using the Xenogen-IVIS Imaging System (Caliper Life Sciences).

***In vitro* iCasp9 safety assay**

Activation of the inducible caspase 9 (iCasp9) safety switch was performed *in vitro* with 2.5, 5, or 10 nM of dimerizer (AP1903), and flow cytometry was used to assess induction of CAR-T cell elimination 24 hours later.

ddPCR copy number assays

Genomic DNA (gDNA) was extracted from GF-CART01 cells using a Qiagen DNeasy Blood and Tissue Kit (Qiagen). Minicircle DNA (positive control) was produced by Aldevron. Before ddPCR, the minicircle DNA was digested for 1 min at 37°C with restriction enzyme Bsrg1. The reaction for ddPCR Copy Number Variation Assay was set up in 20 µl sample volume containing 10 µl of 2 × ddPCR Supermix (no dUTP, BioRad™), 1 µl of FAM-labeled target primers/probe (BioRad™), 1 µl of HEX-labeled reference primers/probe (BioRad™), 0.1 µl of Bsrg1 (Fast digest, NEB™), and 50 ng of gDNA or minicircle DNA (volume 2 µl). Nuclease-free water was used to adjust the

sample to final volume. *RPP30* was used as housekeeping gene. Bsrg1 directly digests in the ddPCR reaction during setup. Droplets were then generated in a QX200 droplet generator (BioRad™) according to manufacturers' instructions with a final volume of 40 µl. DNA amplification was carried out and droplets were analyzed in a QX200 droplet reader (BioRad™). Data was analyzed with QuantaSoft software (BioRad™).

Statistical analysis

Statistical analysis was performed using GraphPad Prism 7 software (GraphPad Software). Two-tailed unpaired t tests were used for comparison of two groups. One-way ANOVA was used for comparison of three or more groups in a single condition. The statistical analysis used for each figure is described in the figure legend. *P* values of less than 0.05 were considered statistically significant, $*p < 0.05$, $**p < 0.01$, and $***p < 0.001$.

Figure Legends

Figure 1. Comparison of perfusion and fed-batch-cultured CAR-T cells. (A) Schematic diagram of GF-CART01 CAR construct. A T2A sequence enables co-expression of iCasp9 and CD20/CD19-targeted scFvs under the EF1α promoter. (B) Characterization of GF-CART01 cells cultured in conventional plates (perfusion) or G-Rex (fed batch) at day 10 after nucleofection. (C) Cytolytic activities of CAR-T cells after 48 or 72 h of co-culture with Raji-GFP/Luc target cells (E:T ratio of 5:1) were assessed by Celigo image cytometry. (B-C) Data represent mean ± SD in 6 healthy donors, n=6. *p<0.05, **p<0.01, ***p<0.001.

Figure 2. Characteristics of GF-CART01 cells. Percentage of (A) CAR^+ and (B) $transposase^+$ (Quantum $pBase^+$) cells were analyzed by flow cytometry on days 1, 8, and 10 after nucleofection. (C) Fold change of GF-CART01 cells after 10 days of culture in G-Rex are shown. (D) Percentage of CD4 and CD8 T cells in the CAR^+ population on day 10 after nucleofection. (E) Distribution of T_N, T_{SCM}, T_{CM}, T_{EM}, and T_{EFF} subsets in the CD4 (upper panel) and CD8 populations (lower panel). (F) Expression of exhaustion markers PD-1, TIM-3, and LAG-3 in GF-CART01 cells. (G) Expression of senescence markers KLRG-1 and CD57 in GF-CART01 cells. (A-G) Data represent mean ± SD in 9 healthy donors, n=9.

Figure 3. *In Vitro* functional analysis of GF-CART01 cells. (A-B) CAR-T cells derived from two healthy donors PBMC-41 and PBMC-40 were assessed for cytotoxicity against Raji-GFP/Luc cells by Celigo image cytometry. Statistical differences were calculated by One-way ANOVA with Tukey multiple comparison, ***p<0.001, **p<0.01, *p<0.05. (C) IFN-γ, (D) TNF-α, and (E) IL-2 secretion by GF-CART01 cells following antigen stimulation was determined by ELISA. Pan-T cells (non-modified cells) served as control group. Data represent mean ± SD, n=3. Statistical differences are calculated by Student's t-test, ***p<0.001.

Figure 4. Anti-tumor activity of GF-CART01 cells in a B-cell lymphoma immunodeficient xenograft mouse model. (A) Schematic diagram of *in vivo* experimental design. (B-C) Bioluminescent imaging was performed to monitor tumor cell persistence (n= 4) and tumor growth were quantified by total flux (photon/s). (D) Kaplan-Meier survival curves for the different treatment groups are shown. (E) Sera from mice were collected on days 2, 5, 8, and 14 after CAR-T cell administration and analyzed for IFN-γ, TNF-α, IL-2, and IL-6 by ELISA. Copy number of (F) luciferase and (G) CAR were determined in mouse blood samples on day 26 after CAR-T cell administration to monitor the presence of CAR^+ T cells and Raji GFP/Luc cells, respectively, in the mouse circulation (n=8 and n=7 for CAR-T(M) and CAR-T(H)). Dotted lines represent the detection limits of qPCR.

Figure 5. Assessment of cancer-patient-derived GF-CART01 cells. T cells derived from healthy donors and cancer patients were nucleofected with GF-CART01. (A) CD8/CD4 ratios were assessed before (PBMC) and after (CAR-T) nucleofection. (B) Distribution of T_N, T_{SCM}, T_{CM}, T_{EM}, and T_{EFF} subsets in $CD4^+$ (upper panel) and $CD8^+$ (lower panel) CAR-T cell populations. *DLBCL, diffuse large B-cell lymphoma; CLL, chronic lymphocytic leukemia; HL, Hodgkin's lymphoma; MM, multiple myeloma*.

Table 1. Comparison of GF-CART01 cells generated from healthy donors and cancer cell patients

CAR-T cells generated from PBMCs of 6 healthy donors and 8 cancer patients were cultured in 24-well G-Rex for 10 days. The cell number of 24-well G-Rex culturing times 50 is equal to cell number of 1L G-Rex culturing ($2.38x10^8$~$1.38x10^9$ cells in 1L G-Rex).

DLBCL: diffuse large B-cell lymphoma; CLL: chronic lymphocytic leukemia; HL: Hodgkin lymphoma; MM: multiple myeloma.

References

1. Larson, R. C. & Maus, M. V. Recent advances and discoveries in the mechanisms and functions of CAR T cells. *Nat. Rev. Cancer* (2021) doi:10.1038/s41568-020-00323-z.
2. Sheth, V. S. & Gauthier, J. Taming the beast: CRS and ICANS after CAR T-cell therapy for ALL. *Bone Marrow Transplant.* **56**, 552–566 (2021).
3. Meir, Y. J. J. & Wu, S. C. Y. Transposon-based vector systems for gene therapy clinical Trials: Challenges and considerations. *Chang Gung Med. J.* **34**, 565–579 (2011).
4. Singh, H., Moyes, J. S. E., Huls, M. H. & Cooper, L. J. N. Manufacture of T cells using the Sleeping Beauty system to enforce expression of a CD19-specific chimeric antigen receptor. *Cancer Gene Ther.* **22**, 95–100 (2015).
5. Brentjens, R. J. *et al.* Eradication of systemic B-cell tumors by genetically targeted human T lymphocytes co-stimulated by CD80 and interleukin-15. *Nat. Med.* **9**, 279–286 (2003).
6. Cronk, R. J., Zurko, J. & Shah, N. N. Bispecific chimeric antigen receptor T cell therapy for b cell malignancies and multiple myeloma. *Cancers (Basel).* **12**, 1–15 (2020).
7. Levin, A. & Shah, N. N. Chimeric antigen receptor modified T cell therapy in B cell non-Hodgkin lymphomas. *Am. J. Hematol.* **94**, S18–S23 (2019).
8. Park, J. H. *et al.* Long-Term Follow-up of CD19 CAR Therapy in Acute Lymphoblastic Leukemia. *N. Engl. J. Med.* **378**, 449–459 (2018).
9. Spiegel, J. Y. *et al.* Outcomes in large B-cell lymphoma progressing after axicabtagene ciloleucel (Axi-cel): Results from the U.S. Lymphoma CAR-T Consortium. *J. Clin. Oncol.* **37**, 7517–7517 (2019).
10. Neelapu, S. S. *et al.* CD19-Loss with Preservation of Other B Cell Lineage Features in Patients with Large B Cell Lymphoma Who Relapsed Post-Axi-Cel. *Blood* **134**, 203–203 (2019).
11. Shah, N. N. *et al.* Bispecific anti-CD20, anti-CD19 CAR T cells for relapsed B cell malignancies: a phase 1 dose escalation and expansion trial. *Nat. Med.* **26**, 1569–1575 (2020).
12. Tong, C. *et al.* Optimized tandem CD19/CD20 CAR-engineered T cells in refractory/relapsed B cell lymphoma. *Blood* **136**, 1632–1644 (2020).
13. Wu, S. C. Y. *et al.* piggyBac is a flexible and highly active transposon as compared to Sleeping Beauty, Tol2, and Mos1 in mammalian cells. *Proc. Natl. Acad. Sci. U. S. A.* **103**, 15008–15013 (2006).
14. Querques, I. *et al.* A highly soluble Sleeping Beauty transposase improves control of gene insertion. *Nat. Biotechnol.* **37**, 1502–1512 (2019).
15. Fraietta, J. A. *et al.* Determinants of response and resistance to CD19 chimeric antigen receptor (CAR) T cell therapy of chronic lymphocytic leukemia. *Nat. Med.* **24**, 563–571 (2018).
16. Gotti, E. *et al.* Optimization of therapeutic T cell expansion in G-Rex device and applicability to large-scale production for clinical use: GMP-compliant polyclonal T cell expansion in G-Rex. *Cytotherapy* **24**, 334–343 (2022).
17. Gagliardi, C., Khalil, M. & Foster, A. E. Streamlined production of genetically modified T cells with activation, transduction and expansion in closed-system G-Rex bioreactors.

Cytotherapy **21**, 1246–1257 (2019).

18. Rafiq, S., Hackett, C. S. & Brentjens, R. J. Engineering strategies to overcome the current roadblocks in CAR T cell therapy. *Nat. Rev. Clin. Oncol.* **17**, 147–167 (2020).
19. Wang, X. *et al.* A transgene-encoded cell surface polypeptide for selection, in vivo tracking, and ablation of engineered cells. *Blood* **118**, 1255–1263 (2011).
20. Wang, Q. *et al.* A transgene-encoded truncated human epidermal growth factor receptor for depletion of anti- B-cell maturation antigen CAR-T cells. *Cell. Immunol.* **363**, 104342 (2021).
21. Micklethwaite, K. P. *et al.* Investigation of product-derived lymphoma following infusion of piggyBac-modified CD19 chimeric antigen receptor T cells. *Blood* **138**, 1391–1405 (2021).
22. Bishop, D. C. *et al.* Development of CAR T-cell lymphoma in 2 of 10 patients effectively treated with piggyBac-modified CD19 CAR T cells. *Blood* **138**, 1504–1509 (2021).
23. Foster, M. C. *et al.* Utility of a safety switch to abrogate CD19.CAR T-cell–associated neurotoxicity. *Blood* **137**, 3306–3309 (2021).
24. Nukala, U., Rodriguez Messan, M., Yogurtcu, O. N., Wang, X. & Yang, H. A Systematic Review of the Efforts and Hindrances of Modeling and Simulation of CAR T-cell Therapy. *AAPS J.* **23**, 1–33 (2021).
25. Turtle, C. J. *et al.* CD19 CAR-T cells of defined CD4+:CD8+ composition in adult B cell ALL patients. *J. Clin. Invest.* **126**, 2123–2138 (2016).
26. Sommermeyer, D. *et al.* Chimeric antigen receptor-modified T cells derived from defined CD8+ and CD4+ subsets confer superior antitumor reactivity in vivo. *Leukemia* **30**, 492–500 (2016).
27. Prommersberger, S. *et al.* CARAMBA: a first-in-human clinical trial with SLAMF7 CAR-T cells prepared by virus-free Sleeping Beauty gene transfer to treat multiple myeloma. *Gene Ther.* **28**, 560–571 (2021).
28. Gattinoni, L., Speiser, D. E., Lichterfeld, M. & Bonini, C. T memory stem cells in health and disease. *Nat. Med.* **23**, 18–27 (2017).
29. Gattinoni, L. *et al.* A human memory T cell subset with stem cell-like properties. *Nat. Med.* **17**, 1290–1297 (2011).
30. Blaeschke, F. *et al.* Induction of a central memory and stem cell memory phenotype in functionally active CD4+ and CD8+ CAR T cells produced in an automated good manufacturing practice system for the treatment of CD19+ acute lymphoblastic leukemia. *Cancer Immunol. Immunother.* **67**, 1053–1066 (2018).
31. Li, Y. *et al.* Targeting IL-21 to tumor-reactive T cells enhances memory T cell responses and anti-PD-1 antibody therapy. *Nat. Commun.* **12**, 1–13 (2021).
32. Ghassemi, S. *et al.* Rapid manufacturing of non-activated potent CAR T cells. *Nat. Biomed. Eng.* **6**, 118–128 (2022).
33. Arcangeli, S. *et al.* Next-Generation Manufacturing Protocols Enriching TSCM CAR T Cells Can Overcome Disease-Specific T Cell Defects in Cancer Patients. *Front. Immunol.* **11**, (2020).
34. Funk, C. R. *et al.* PI3Kδ/γ inhibition promotes human CART cell epigenetic and metabolic reprogramming to enhance antitumor cytotoxicity. *Blood* **139**, 523–537 (2022).
35. Yan, C. *et al.* Memory stem T cells generated by Wnt signaling from blood of human renal

clear cell carcinoma patients. *Cancer Biol. Med.* **16**, 109–120 (2019).

36. Joedicke, J. J. *et al.* Accelerating clinical-scale production of BCMA CAR T cells with defined maturation stages. *Mol. Ther. - Methods Clin. Dev.* **24**, 181–198 (2022).
37. Herndler-Brandstetter, D. *et al.* KLRG1+ Effector CD8+ T Cells Lose KLRG1, Differentiate into All Memory T Cell Lineages, and Convey Enhanced Protective Immunity. *Immunity* **48**, 716-729.e8 (2018).
38. Liu, Q., Sun, Z. & Chen, L. Memory T cells: strategies for optimizing tumor immunotherapy. *Protein Cell* **11**, 549–564 (2020).
39. Noviello, M. *et al.* Bone marrow central memory and memory stem T-cell exhaustion in AML patients relapsing after HSCT. *Nat. Commun.* **10**, 1–15 (2019).
40. Vormittag, P., Gunn, R., Ghorashian, S. & Veraitch, F. S. A guide to manufacturing CAR T cell therapies. *Curr. Opin. Biotechnol.* **53**, 164–181 (2018).
41. Brentjens, R. J. *et al.* Safety and persistence of adoptively transferred autologous CD19-targeted T cells in patients with relapsed or chemotherapy refractory B-cell leukemias. *Blood* **118**, 4817–4828 (2011).
42. Porter, D. L. *et al.* Chimeric antigen receptor T cells persist and induce sustained remissions in relapsed refractory chronic lymphocytic leukemia. *Sci. Transl. Med.* **7**, (2015).
43. Dai, H. *et al.* Tolerance and efficacy of autologous or donor-derived T cells expressing CD19 chimeric antigen receptors in adult B-ALL with extramedullary leukemia. *Oncoimmunology* **4**, (2015).
44. W.-K. Hua, *et al.*, *Quantum pBac*: An effective, high-capacity *piggyBac*-based gene integration vector system for unlocking gene therapy potential. (*Manuscript in preparation*).
45. Y.-C. Chen, *et al.*, *Quantum CART* (*qCART*), a *piggyBac*-based system for development and production of virus-free multiplex CAR-T cell therapy (*Manuscript in preparation*).

Figure 1

A

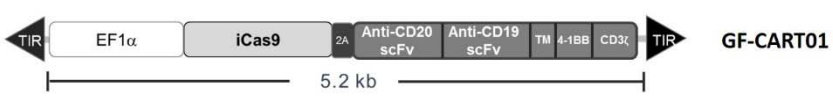

B

Culture Vessel	Conventional Plate (perfusion)	G-Rex (fed batch)
% CAR⁺ T cells	51%* (44%~61%, n=6)	46%* (42%~49%, n=6)
Expansion capacity of CAR⁺ T cells	836 fold* (406~2090 fold, n=6)	189 fold* (139~262 fold, n=6)
Distribution of T cell subsets in CAR⁺ T cells	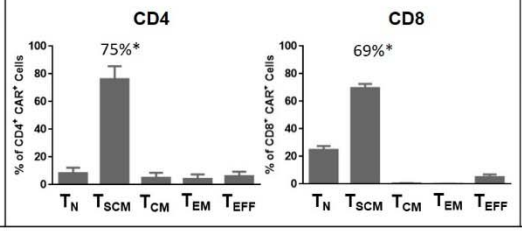	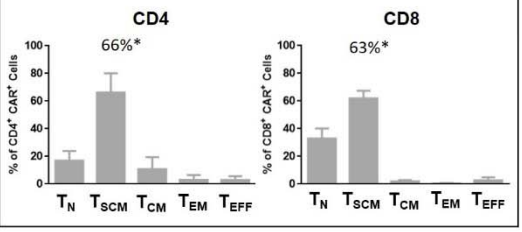

*median

C

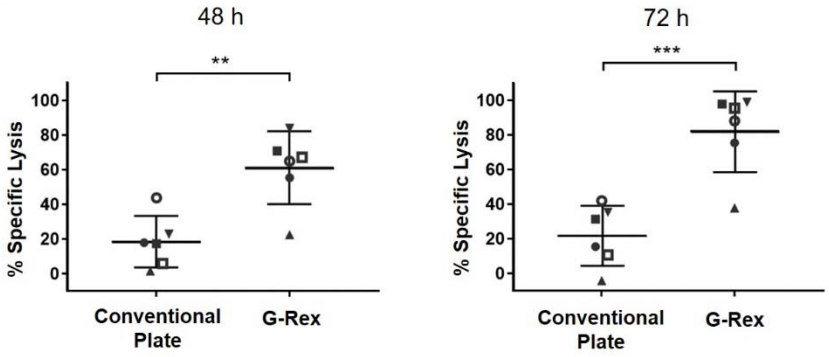

Figure 2

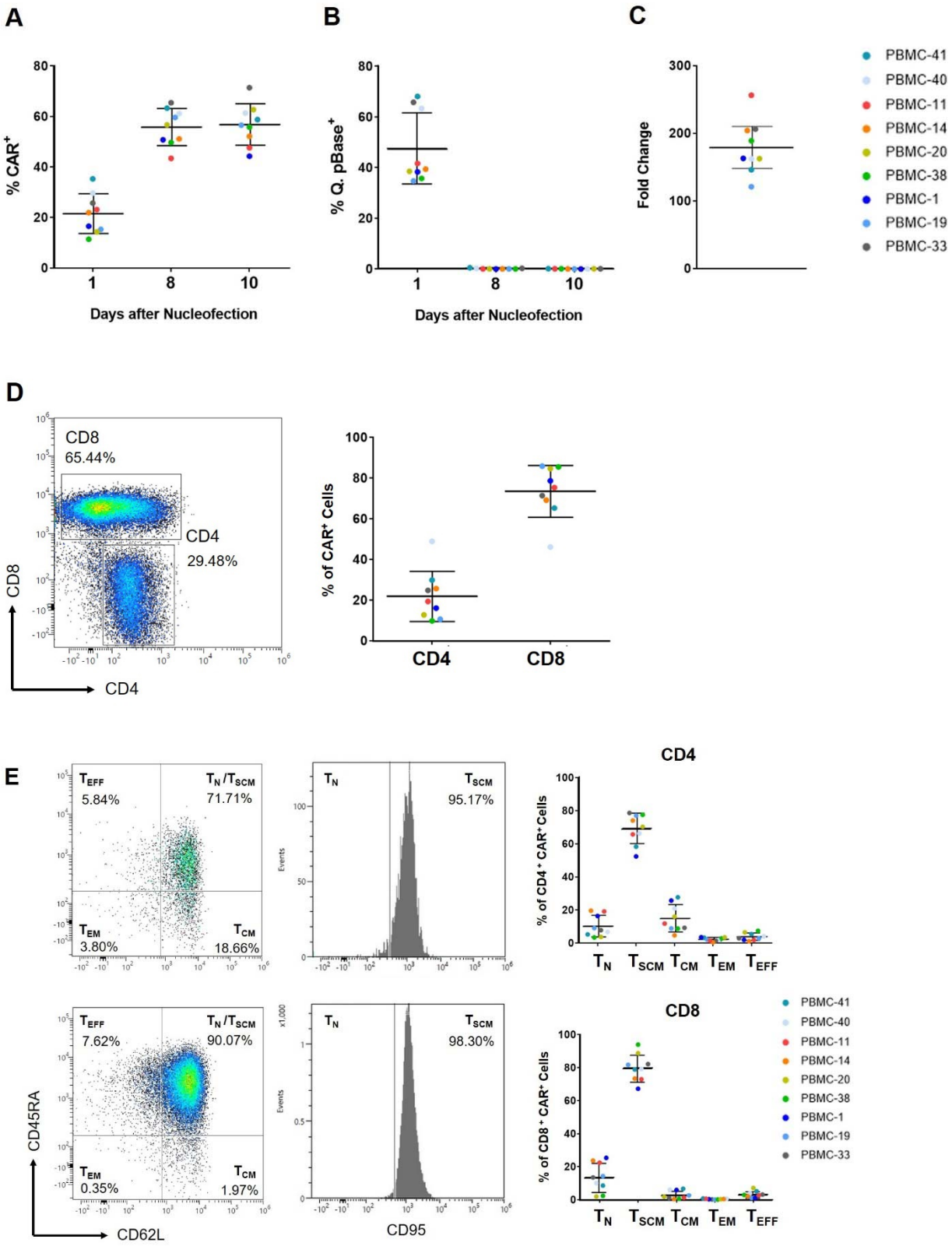

Figure 2 (con'd)

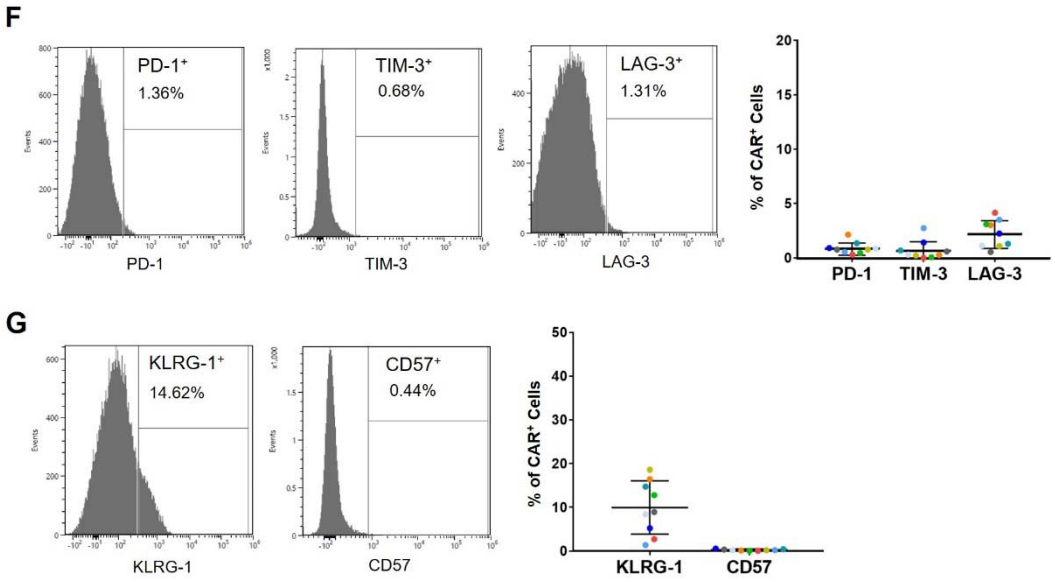

Figure 3

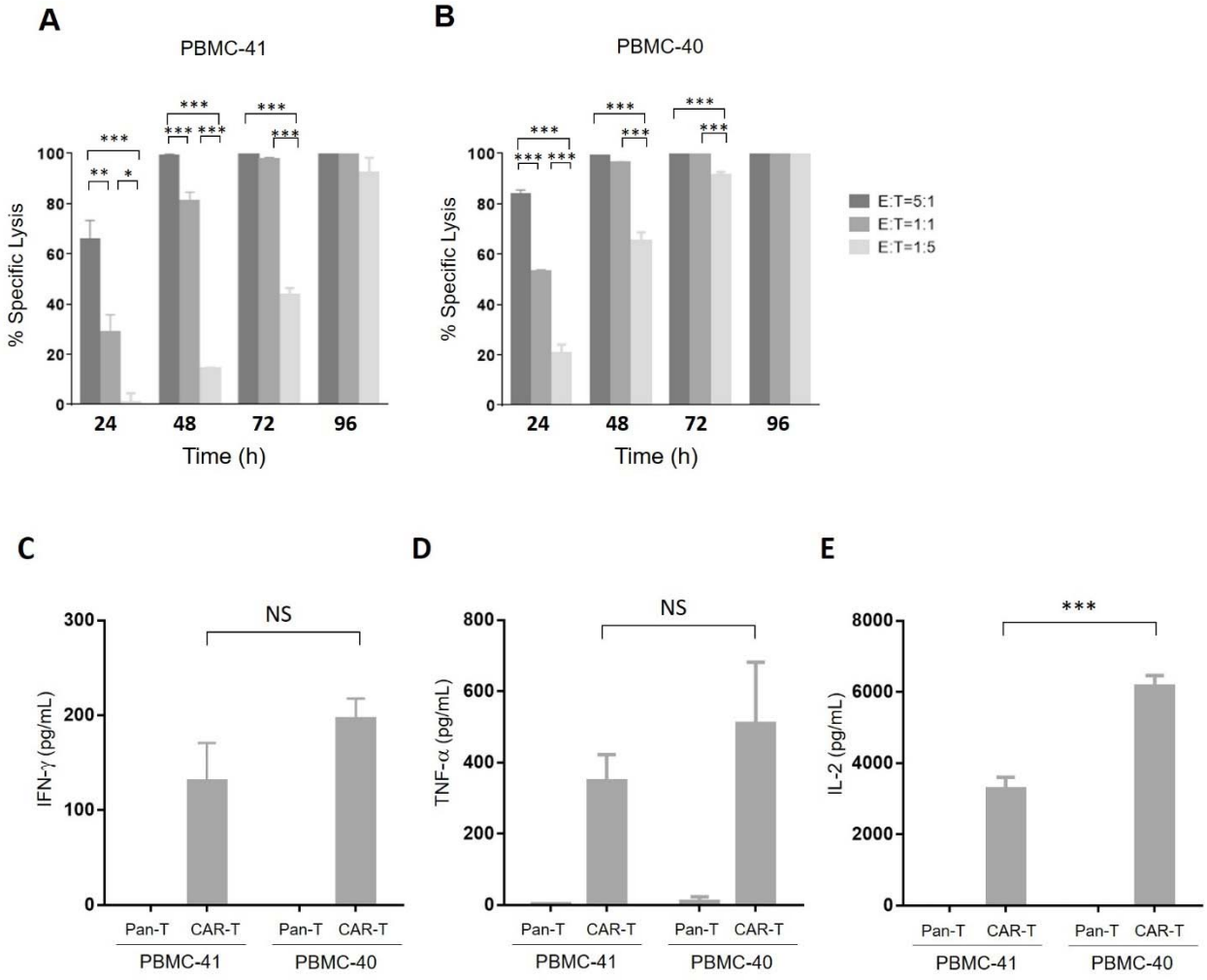

Figure 4

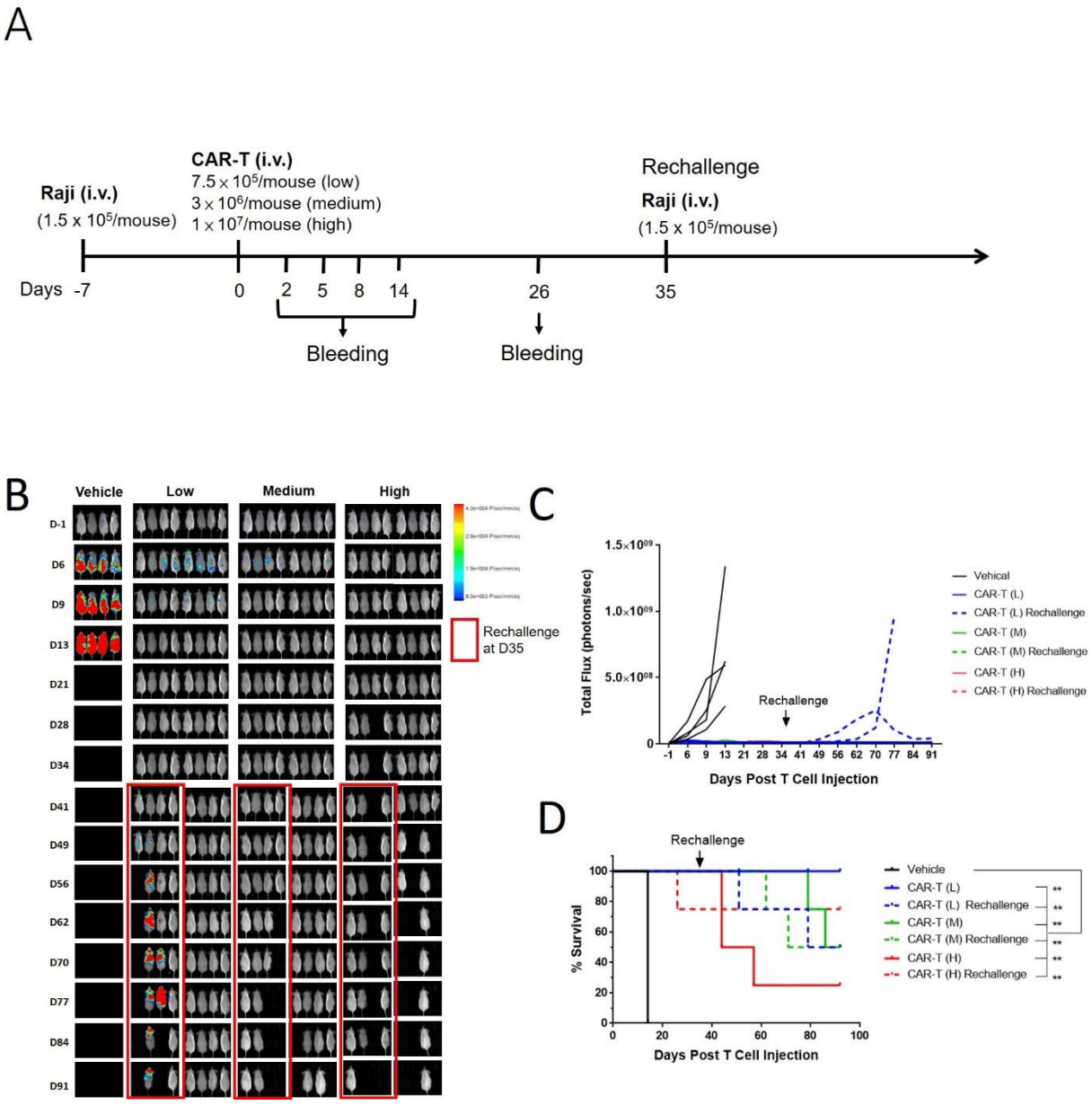

Figure 4 (con'd)

E

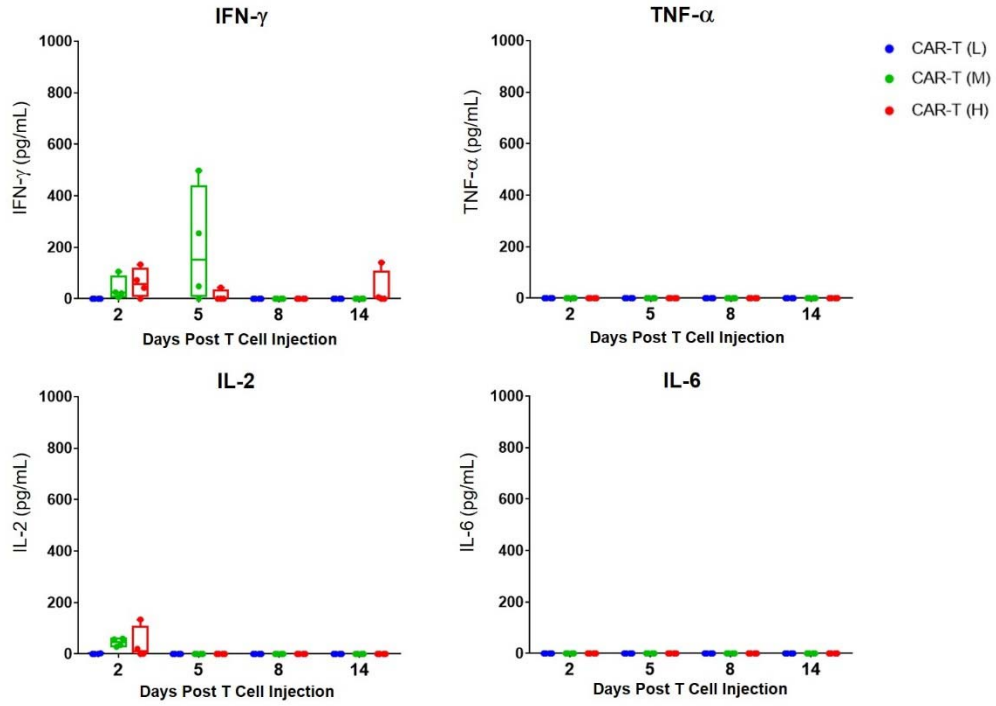

F

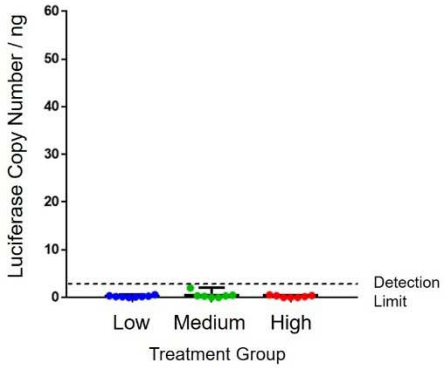

G

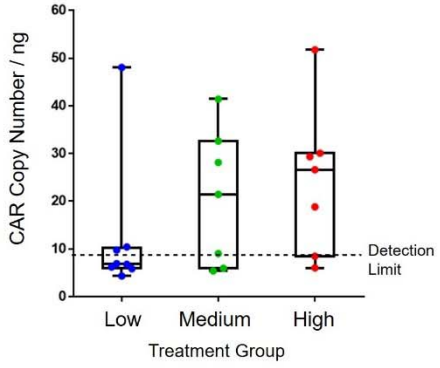

Figure 5

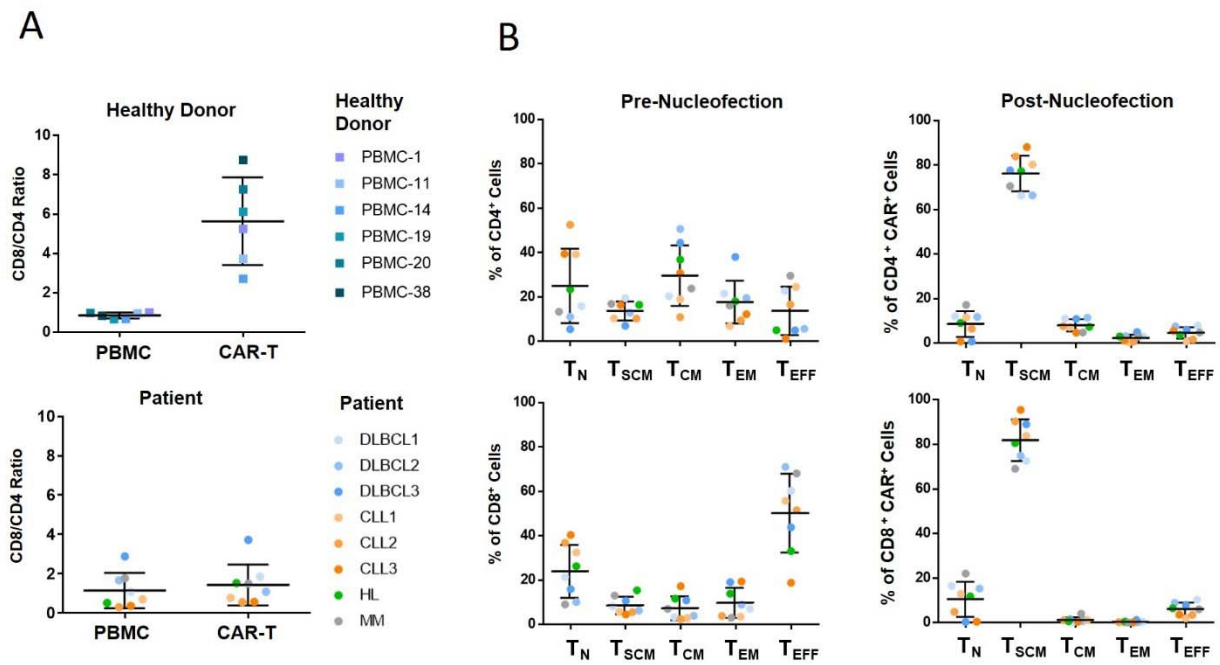

Table 1

Table 1. Comparison of GF-CART01 cells generated from healthy donors and cancer patients

Disease		Healthy Donor	DLBCL1	DLBCL2	DLBCL3	CLL1	CLL2	CLL3	HL	MM
Copy Number		1.85-3.47	2.51	5.46	2.21	3.36	2.81	3.76	2.04	1.82
% CAR$^+$		32.5–49.6	26.3	50.1	34.23	40.6	33.4	53.22	26.2	19.9
Fold Expansion		43.54–157.55	67.22	67.3	60.38	104.6	58.0	198.96	149.75	139.35
Cell Number (x10^6)		17.34–50.60	7.29	4.95	5.8	15.8	7.71	4.58	24.08	27.54
B cell (CD19$^+$)		0.01-0.36	0.77	1.18	0.35	0	0	0.61	0	0
NK cell (CD3$^-$, CD56$^+$)		0.04-0.27	0.06	2.69	0.63	0.03	0.02	0.02	0.08	0.05
% Exhaustion Markers	PD-1	0.40–1.96	5.4	4.2	4.2	1.0	2.4	6.0	1.7	7.8
	TIM-3	0.10–5.34	1.8	3.0	2.0	1.4	2.3	2.4	1.4	1.1
	LAG-3	0.90–7.00	9.9	12.4	22.8	3.2	4.0	2.6	2.4	2.6
% Senescence Markers	KLRG-1	2.24–14.61	11.8	14.7	8.2	2.8	4.2	6.1	4.1	5.3
	CD57	0.03–0.68	5.8	1.5	2.5	1.1	1.8	0.6	1.1	1.3
Potency (% Lysis) (fresh cells, E:T=5, 48 h)		89.74–95.38	99.66	99.7	99.7	99.88	99.45	99.07	98.96	99.42
Potency (% Lysis) (frozen cells, E:T=5, 48 h)		44.99–61.96	73.35	74.21	75.21	84.30	75.70	45.46	77.49	70.31